Optical and magnetic properties of some XMnSb and Co$_2$YZ Compounds: *ab initio* calculations

Selami Palaz[1], Husnu Koc[2], Haci Ozisik[3], Engin Deligoz[4], Amirullah M. Mamedov[*,5,6], and Ekmel Ozbay[5]

[1] Faculty of Science and Letters, Department of Physics, Harran University, 63000 Sanliurfa, Turkey

[2] Faculty of Arts and Sciences, Department of Physics, Siirt University, 56100 Siirt, Turkey

[3] Education Faculty, BOTE Department, Aksaray University, 68100 Aksaray, Turkey

[4] Faculty of Science and Letters, Department of Physics, Aksaray University, 68100 Aksaray, Turkey

[5] Nanotechnology Research Center, Bilkent University, 06800 Ankara, Turkey

[6] International Scientific Center, Baku State University, Baku, Azerbaijan

* Corresponding author: e-mail **mamedov@bilkent.edu.tr**, Phone: +90-312-290-1966, Fax: +90-312-266-4042

In present work, our research is mainly focused on the electronic structures, optical, and magnetic properties of XMnSb (X = Ni, Cu, Pd), Co$_2$YZ (Y = Ti; Z=Si, Ge, Sn), and Co$_2$YZ (Y =Mn; Z=Al, Ga, Si) Heusler compounds by using *ab initio* calculations within the generalized gradient approximation. The calculations are performed by using the Vienna *ab initio* simulation package based on the density functional theory. The band structure of these Heusler alloys for majority spin and minority spin were calculated and the majority spin states cross the Fermi level and thus have the metallic character, while the minority spin states open the band gaps around the Fermi level and thus have the narrow-band semiconducting nature. We also find that these Heusler compounds have the indirect band gaps in the minority spin channel. The real and imaginary parts of dielectric functions and hence the optical functions such as energy-loss function, the effective number of valance electrons and the effective optical dielectric constant for XMnSb and Co$_2$YZ compounds were also calculated. In addition, we also show the variations of the total magnetic moment per f.u. and minority spin gap width of these compounds with optimized lattice constants: minority spin gap width decreases with increasing the lattice constants.

1 Introduction The Heusler compounds is a ferromagnetic metal compounds based on a Heusler phase. They have interesting electronic and magnetic properties. Because of these properties, the Heusler compounds have attracted for the design of single-spin electron sources and spin injectors in the field of magneto-electronics and related technological applications [1, 2, 3]. The half-Heusler phases XYZ, comprising three interpenetrating fcc lattices, constitute an important class of materials with particular regard to their magnetic properties [4]. Ternary Heusler and half-Heusler compounds have the chemical formula X$_2$YZ or XYZ, where X and Y are transition or rare earth metals and Z a heavy element. In some cases, Y is replaced by a rare earth element [5]. Half-Heusler compounds XYZ, also called semi-Heusler compounds, crystallize in the MgAgAs-type structure (see Table 1), in the space group F-43 m [4].

NiMnSb, CuMnSb, and PdMnSb are member of the family of Heusler compounds. Otto et al. have investigated of the crystal structure the microstructure and the magnetic properties of the inter-metallic compounds NiMnSb and CuMnSb [6]. They have reported that magnetic properties show an effective paramagnetic moment which differs from the value corresponding to the saturation moment at 0 K. This effect is attributed to a decrease of the conduction electron spin polarisation at high temperature. PdMnSb compound is synthesized by Webster and Ziebeck [7].

In the present work, by means of a DFT approach we examined the series of Heusler alloys XMnSb and Co$_2$YZ assuming they crystallize in the typical C1$_b$ and L2$_1$ structures. For all these compounds we derived structural, mechanical, electronic, optical properties. Consequently, the primary purpose of this work is to provide some

Table 1 Crystallographic parameters of C1$_b$ and L2$_1$ structures.

C1$_b$	SPG. F-43m (216)				L2$_1$	SPG. Fm-3m (225)		
X	4d	3/4	3/4	3/4	Co	4c	1/4	1/4	1/4
Mn	4b	1/2	1/2	1/2	Y	4b	1/2	1/2	1/2
Sb	4a	0	0	0	Z	4a	0	0	0
	4c	1/4	1/4	1/4					

additional information to the existing data on the physical properties of XMnSb and Co$_2$YZ compounds by using the *ab initio* total energy calculations.

2 Methodology The *ab initio* calculation based on DFT was used with the aid of the VASP [8, 9, 10] program. The exchange and correlation potentials were Perdew-Burke-Ernzerhof method [11] based on generalized gradient approximation (GGA). The plane wave cutoff energy in the wave vector K space was 500 eV. We have performed the Brillouin-Zone integration by using $9 \times 9 \times 9$ gamma centered special Monkhorst-Pack k-points [12]. The investigated properties of XMnSb and Co$_2$YZ are calculated using the primitive cells (Z = 1). When the total energy was stabilized within 10^{-1} eV, the force acting on each atom of the cell after optimization was less than 0.001 eV Å^{-1}, the residual stresses of the cell was less than 0.001 GPa and the tolerance offset was less than 10^{-5} Å. The elastic constants are calculated by the efficient stress-strain method as implemented in the VASP code [13]. The optical properties were obtained complex dielectric function $\varepsilon(\omega) = \varepsilon_1(\omega) + i\varepsilon_2(\omega)$ where the details explained in Refs. [14, 15].

3 Results and discussion

3.1 Crystal structures We have examined XMnSb and Co$_2$YZ compounds with the half-Heusler and Heusler structure, respectively. First, a structural optimization was performed for these compounds to determine whether the experimental lattice parameter minimizes the total energy. The calculated equilibrium lattice constant, total energy, ground state volume, and total magnetic moments values are given Table 2. It was found that the optimized lattice parameter and magnetic moments from the calculation agrees very well with experimental values [6, 7]. Co$_2$MnSi has the highest magnetic moment and Co$_2$TiSn has the lowest one. We also show the variations of the total magnetic moment per f.u. and minority spin gap width of these compounds with optimized lattice constants: minority spin gap width decreases with increasing the lattice constants.

3.2 Mechanical properties The estimated independent elastic constants are tabulated in Table 3. To our knowledge, there are no experimental or theoretical data available for elastic constants except Co$_2$MnSi The calculated elastic constants satisfy Born criteria [20, 21, 22]. Therefore, it can be said that, XMnSb and Co$_2$YZ compounds for considered structure are mechanically stable.

Table 2 The calculated equilibrium lattice constant (a in Å), ground state volume (V_0 in Å^3/f.u.), total energy (E_0 in eV/f.u.) and total magnetic moments (M in μB/f.u.) values.

material	a	V_0	E_0	M_T	references
NiMnSb	5.900	51.35	−19.229	3.96	present
	5.927				exp. [6]
	5.909			3.85	exp. [7]
CuMnSb	4.965	56.21	−16.574	4.09	present
PdMnSb	6.207	59.79	−19.122	3.97	present
	6.248			3.95	exp. [7]
Co$_2$TiSi	5.742	47.32	−29.962	2.06	present
Co$_2$TiGe	5.835	49.67	−28.386	2.05	present
Co$_2$TiSn	6.083	56.28	−27.192	1.15	present
Co$_2$MnAl	5.689	46.03	−28.194	4.02	present
	5.755				exp. [16]
	5.689				GGA [17]
Co$_2$MnGa	5.709	46.51	−26.884	4.10	present
	5.77				exp. [18]
Co$_2$MnSi	5.621	44.40	−30.213	5.00	present
	5.654			5.00	exp. [19]
	5.645			5.01	GGA [19]

Isotropic bulk moduli, shear moduli, Young's moduli, Poisson's ratios, B/G ratios, and Debye temperatures are calculated by using Voigt-Reuss-Hill approach [23, 24, 25]. The results are tabulated in Table S1 (in Supporting information). It shows that the calculated values of bulk moduli, shear moduli, Young's moduli of Co$_2$YZ are higher than XMnSb. We note that the B/G values are all higher than 1.75. Therefore, the studied systems in its all forms can be classified as ductile materials [26]. Our calculated values of Poisson's ratio vary from 0.27 to 0.40 for these compounds. Thus, indicating strong metalic contribution in the intra-atomic bonding for these compounds.

3.3 Electronic properties The electronic structure plays an important role in determining the magnetic properties of the Heusler compounds. The band structure of along the principal symmetry directions have been calculated by using the equilibrium lattice constants as shown in Table 2. The band structure of the XMnSb and Co$_2$YZ Heusler alloys for majority spin (spin-up) and

Table 3 The calculated elastic constants (C_{ij} in GPa).

material	C_{11}	C_{12}	C_{44}	references
NiMnSb	170.9	82.7	54.7	present
CuMnSb	105.6	63.9	39.2	present
PdMnSb	114.5	88.0	27.8	present
Co$_2$TiSi	294.7	159.7	122.8	present
Co$_2$TiGe	265.0	151.9	114.2	present
Co$_2$TiSn	243.5	129.8	98.3	present
Co$_2$MnAl	270.2	151.6	150.1	present
Co$_2$MnGa	256.9	165.6	142.3	present
Co$_2$MnSi	312.0	177.9	139.5	present
	290–363	126–203	102–170	theoretical [19]

Phys. Status Solidi C 14, No. 6 (2017)

Contributed

Article

(3 of 4) 1600182

minority spin (spin-down) were calculated. The calculated band structures and total density of states are shown in Fig. 1 for Co$_2$TiZ (Z = Si, Ge, Sn) compound (see Figs. S1 and 2 for XMnSb (X = Ni, Cu, Pd) and Co$_2$MnZ (Z = Al, Ga, Si) compounds in Supporting information). It is seen that for these compounds, the majority spin states cross the Fermi level and thus have the metallic and semimetallic characters, while the minority spin states open the band gaps around the Fermi level and thus have the narrow-band semiconducting nature.

3.4 Optical properties We have first calculated the real and imaginary part of $\varepsilon(\omega) = \varepsilon_1(\omega) + i\varepsilon_2(\omega)$ complex dielectric function using the Kramers–Kroning relations [27]. The optical constant such as energy-loss function, the effective number of valance electrons and the effective optical dielectric constant have been calculated with the help of the real and imaginary part of dielectric function for these compounds. The obtained results showed manner similar to our recent works [28].

The energy values of ε_1 that decreasing $(d\varepsilon_1)/(dE < 0)$ and increasing $(d\varepsilon_1)/(dE > 0)$ are zero are 2.18 and 15.84 eV for Co$_2$MnAl compound, 6.60 and 20.92 eV for Co$_2$MnSi compound, and 2.28 and 22.00 eV for Co$_2$MnGa compound. These values that the ε_1 are zero are points reduced of the reflections, and show that the polarization disappears. The maximum peak values of ε_2 are 1.13, 2.28, and 7.28 eV for Co$_2$MnAl compound, 2.45, 8.40, and 11.10 eV for Co$_2$MnSi compound, and 1.30, 6.30, and 9.17 eV for Co$_2$MnGa compound. These values show how much the electromagnetic wave polarizes the system, and corresponds to the electronic transitions from the valance band to the conduction band. Furthermore, 0–1.3 eV, 0–0.6 eV, and 0–0.7 eV energy region for Co$_2$MnSi, Co$_2$MnAl, and Co$_2$MnGa compounds, respectively is the region where dispersion and transparency are low. This energy region corresponds to the region beginning of the transition between the bands. The 1.4–10 eV energy region for these compounds is the region where the transitions between the bands are very intense. The 2–10 eV energy region has reduced transitions between the bands. The energy region above 12 eV also corresponds to the collective vibration of valance electrons. This energy region defined as plasma oscillations is described by the energy loss function (L). The sharp maxima in the energy-loss function are associated with the existence of plasma oscillations (as an example see Fig. 2).

The optical data for XMnSb show that in the limit of infrared or visible region of the spectrum that has been studied the values of the real part of the dielectric constant lie near zero (as for Co$_2$YZ). This means that the negative contribution from the accelerating mechanism of absorption is quite small and is compensated by the positive contribution from the real and virtual interband transitions of electrons. Such a behavior of the ε_1 function indicates the low concentration of conduction electrons in XMnSb. The presence of a Drude component in the dielectric functions of X$_2$YZ (L2$_1$ phase) permitted us to determine the parameters of free electrons-plasma frequency of conduction electrons E$_{pl}$ = 18.3 eV and the effective number of free electrons $-N_{eff}$ = 2.4 × 10^{22} cm^{-3}. The low values of N_{eff} indicate the formation of a pseudogap in the energy band spectrum of Co$_2$YZ. In the case of XYZ, the zero values of ε_1 prevent making corresponding estimates for N_{eff}. However, it is reasonable to explain the observed behavior of the dielectric
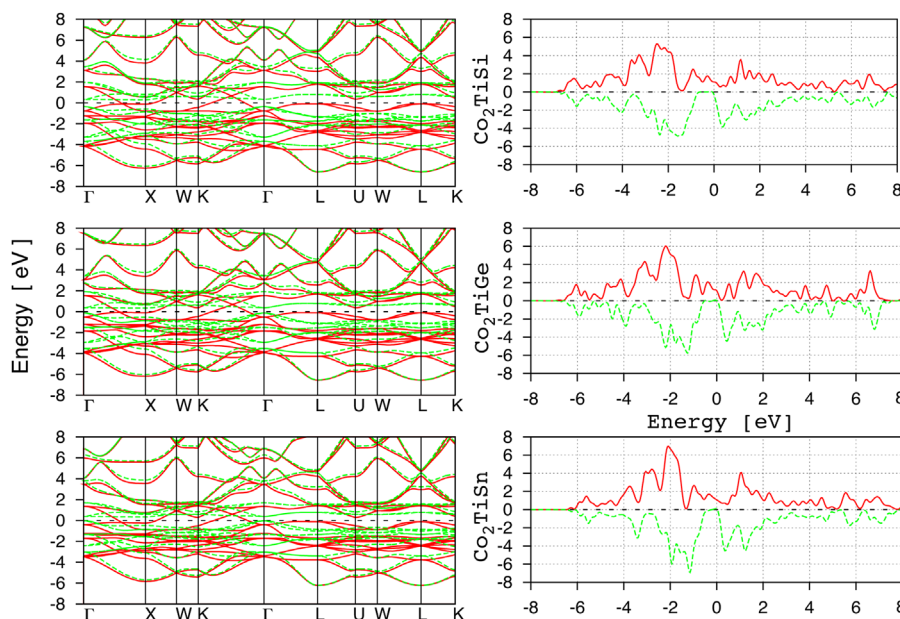

Figure 1 Electronic band structure and total density of states of the Co$_2$TiZ (Z = Si, Ge, Sn) compounds. Solid and dashed lines refer the spin-up and spin-down states, respectively. Find the figures for XMnSb and Co$_2$MnZ (Z = Al, Ga, Si) compound in Supporting information (Figs. S1 and 2).
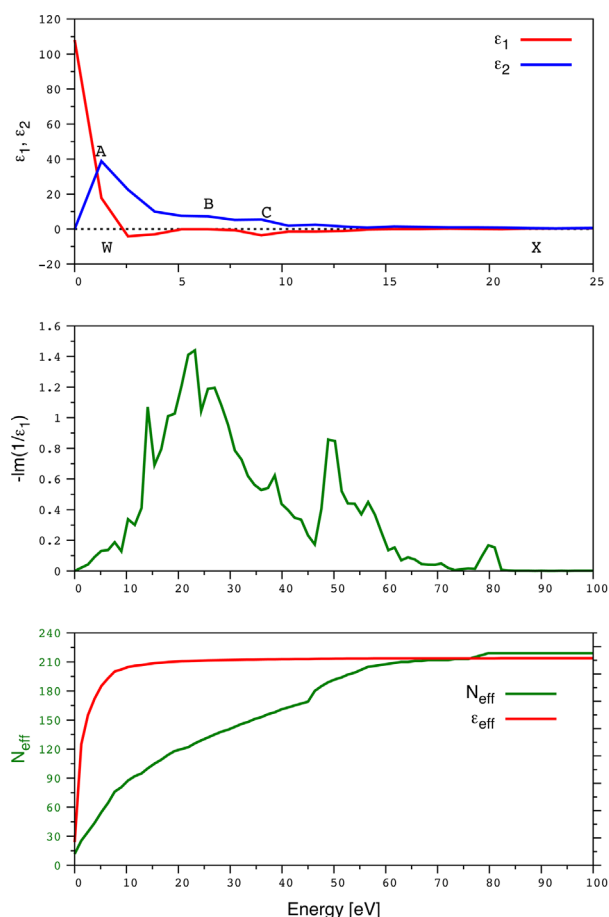
Figure 2 (a) Reel and imaginary parts of dielectric functions, (b) Electron energy-loss spectrum, and (c) Effective number of electrons participating in the interband transitions and effective optical dielectric constant for the Co_2MnGa.

properties of XMnSb by the formation of a deeper pseudogap in the density of states as compared to Co_2YZ. Our results concerning the low-energy interband absorption indicate a weak "growing-in" of the gap in the density of states, which was predicted theoretically for the $C1_b$ phase of XMnSb. Thus, we can conclude that there occurs a loss of the half-metallic character of the energy band spectrum of XMnSb in the case of the vacancy-containing phase with the structure of the $L2_1$ type.

4 Conclusions In this work, we have investigated structural, mechanical, magnetic, electronic, and optical properties of some Co_2YZ and XMnSb Heusler alloys. The estimated lattice parameters are agreement with experimental data. The results of elastic constants reveal all compounds are mechanically stable. The traditional B/G ratio indicates that considered compounds possess ductile nature. The electronic structure calculations show that the majority spin states cross the Fermi level and thus have the metallic character, while the minority spin states open the band gaps around the Fermi level and thus have the narrow-band semiconducting nature. We also find that these

Heusler compounds have the indirect band gaps E_g in the minority spin channel. Finally, optical properties were studied. The relations of the optical properties to the interband transitions were also discussed.

Supporting Information Additional supporting information may be found in the online version of this article at the publisher's web-site.

References

[1] J. H. Park, E. Vescovo, H. J. Kim, C. Kwon, R. Ramecsh, and T. Venkatesan, Nature **392**, 794 (1998).
[2] S. J. Hashemifar, P. Kratzer, and M. Scheffler, Phys. Rev. Lett. **94**, 096402 (2005).
[3] SA. Wolf, DD. Awschalom, RA. Buhrman, JM. Daughton, S. vonMolnar, ML. Roukes, AY. Chtchelkanova, and DM. Treger, Science **294**, 1488 (2001).
[4] H. C. Kandpal, C. Felser, and R. Seshadri, J. Phys. D: Appl. Phys. **39**, 5 (2006).
[5] H. C. Kandpal, G. H. Fecher, C. Felser, and G. SchÃ¶nhense, Phys. Rev. B **73**, 094422 (2006).
[6] M. J. Otto, R. A. M. van Woerden, P. J. van der Valk, J. Wijngaard, C. F. van Bruggen, C. Haas, and K. H. J. Buschow, J. Phys.: Condens. Matter **1**, 2341 (1989).
[7] P. J. Webster and K. R. A. Ziebeck, Landolt Boernstein Neue Series Group III vol 19C (Springer, Berlin, 1988).
[8] G. Kresse and J. Furthmuller, Comp. Mater. Sci. **6**, 15 (1996).
[9] P. E. Blochl, Phys. Rev. B **50**, 17953 (1994).
[10] G. Kresse and J. Furthmuller, Phys. Rev. B **54**, 11169 (1996).
[11] J. P. Perdew, K. Burke, and M. Ernzerhof, Phys. Rev. Lett. **77**, 3865 (1996).
[12] H. J. Monkhorst and J. D. Pack, Phys. Rev. B **13**, 5188 (1976).
[13] Y. L. Page and P. Saxe, Phys. Rev. B **65**, 104104 (2002).
[14] N. Korozlu, K. Colakoglu, E. Deligoz, and Y. O. Ciftci, Opt. Commun. **284**, 186 (2011).
[15] M. Gajdos, K. Hummer, G. Kresse, J. FurthmÃ¼ller, and F. Bechstedt, Phys. Rev. B **73**, 045112 (2006).
[16] R. Y. Umetsu, K. Kobayashi, A. Fujita, R. Kainuma, and K. Ishida, J. Appl. Phys. **103**, 07D718 (2008).
[17] X. Zhu, E. Jiang, Y. Dai, and C. Luo, J. Alloys Compd. **632**, 528 (2015).
[18] S. Finizio, A. Kronenberg, M. Vafaee, M. Foerster, K. Litzius, A. Lucia, T. O. Mentes, L. Aballe, B. KrÃ¼ger, M. Jourdan, and M. Klaui, New J. Phys. **17**, 083030 (2015).
[19] A. Akriche, H. Bouafia, S. Hiadsi, B. Abidri, B. Sahli, M. Elchikh, M. A. Timaoui, and B. Djebour, J. Magn. Magn. Mater. **422**, 13 (2017).
[20] M. Born, Proc. Cambridge Philos. Soc. **36**, 160 (1940).
[21] H. Ozisik, K. Colakoglu, H. B. Ozisik, and E. Deligoz, Comput. Mater. Sci. **50**, 349 (2010).
[22] E. Ateser and H. B. Ozisik, Mod. Phys. Lett. B **26**, 1250107 (2012).
[23] W. Voigt, Lehrbuch der Kristallpysik (Taubner, Leipzig, 1928) p. 29.
[24] A. Reuss and Z. Angew, Math. Mech. **9**, 49 (1929).
[25] R. Hill, Proc. Phys. Soc. London **65**, 349 (1952).
[26] S. F. Pugh, Phil. Mag. Ser. **45**, 823 (1954).
[27] H. R. Philipp and H. Ehrenreich, Phys Rev. **129**, 1550 (1963).
[28] H. Koc, H. Ozisik, E. Deligoz, A. M. Mamedov, and E. Ozbay, J. Mol. Model. **20**, 1 (2014).